Supporting Information for

Anion binding in aqueous media by a tetra-triazolium macrocycle

Nicholas G. White,[a] Sílvia Carvalho,[b] Vítor Félix,[b] & Paul D. Beer[a]*

[a] Chemistry Research Laboratory, Department of Chemistry, University of Oxford,
South Parks Road, Oxford, OX1 3TA, United Kingdom.
Fax: +44 1865 272690.
Tel: +44 1865 285142
E-mail: paul.beer@chem.ox.ac.uk

[b] Departamento de Química, CICECO and Secção Autónoma de Ciências da Saúde,
Universidade de Aveiro, 3810-193 Aveiro, Portugal

Contents:

2. NMR Titrations Protocols

3. Spectra for New Compounds

9. Gas Phase Molecular Modelling

11. Experimental Details for Molecular Modelling

14. References

NMR Titration Protocols

Initial sample volumes were 0.50 mL and concentrations were 2.0 mmol L^{-1} of host. Solutions (100 mmol L^{-1}) of anions as their tetrabutylammonium salts were added in aliquots, the samples thoroughly shaken and spectra recorded. Spectra were recorded at 0, 0.2, 0.4, 0.6, 0.8, 1.0, 1.2, 1.4, 1.6, 1.8, 2.0, 2.5, 3.0, 4.0, 5.0, 7.0 and 10 equivalents. Stability constants were obtained by analysis of the resulting data using the WinEQNMR2[S1] computer program, following the triazole or triazolium C-H protons in all cases.

^{1}H and ^{13}C NMR Spectra of New Compounds

Propyl-linked bis-azide 6

^{1}H NMR (300 MHz, 293 K, CDCl$_3$):

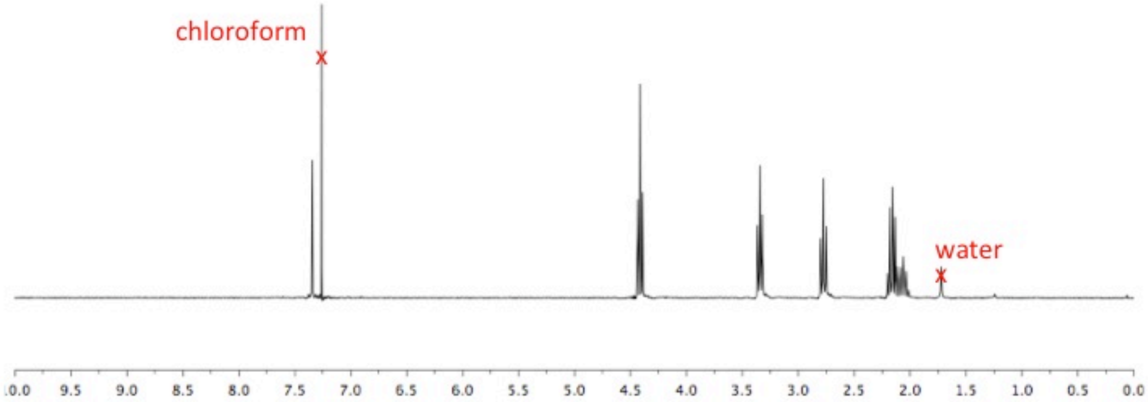

^{13}C NMR (75.5 MHz, 293 K, CDCl$_3$):

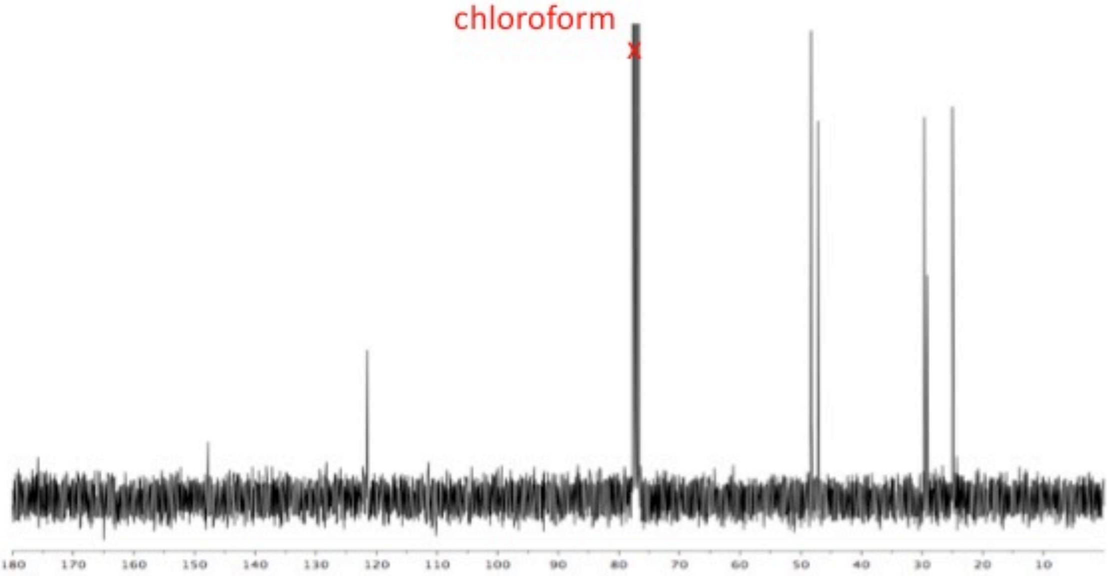

Phenyl-linked bis-azide 5

^{1}H NMR (300 MHz, 293 K, $CDCl_3$):

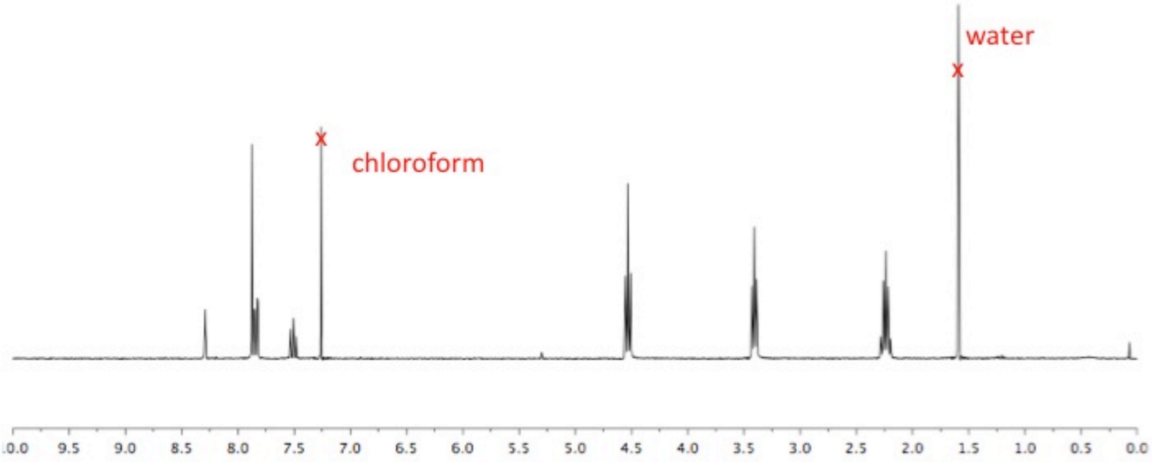

^{13}C NMR (75.5 MHz, 293 K, $CDCl_3$):

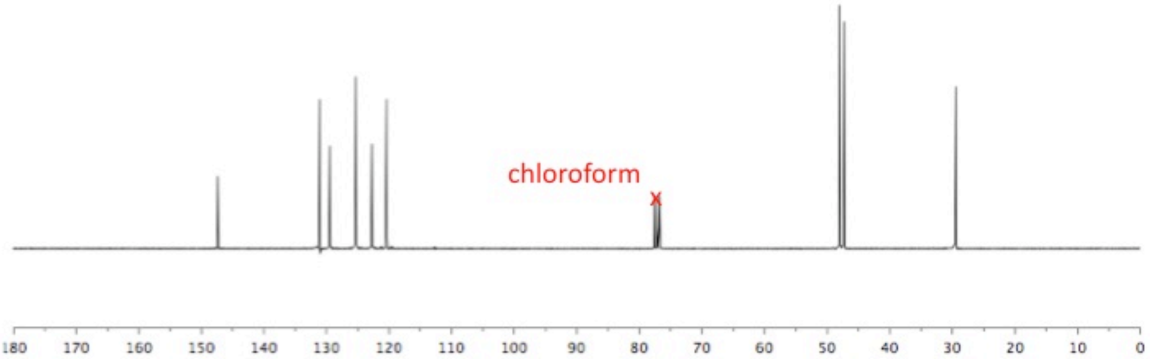

Propyl-linked tetra-triazole macrocycle 1

^{1}H NMR (500 MHz, 293 K, d_6-DMSO):

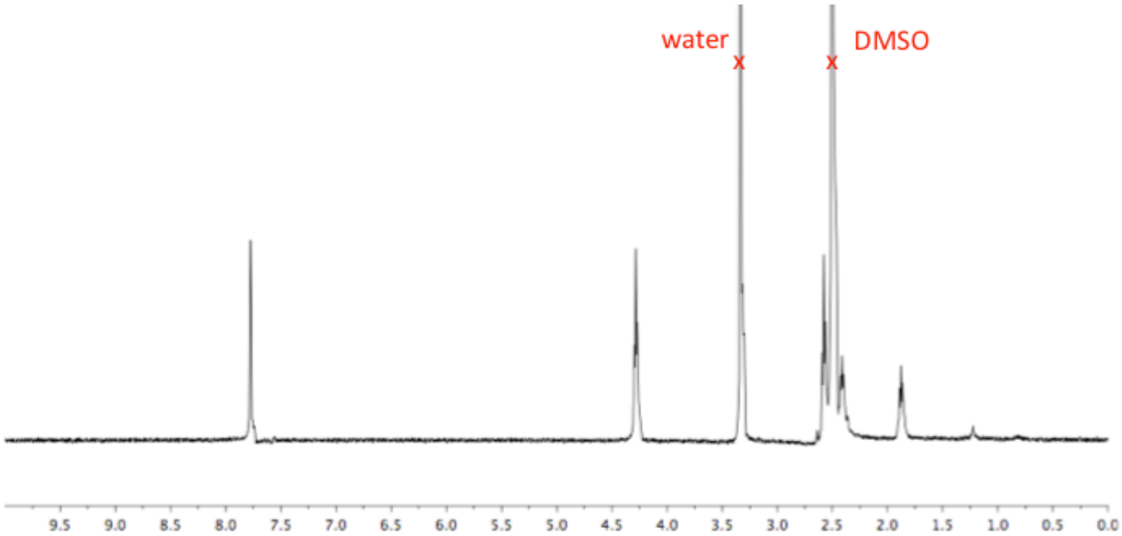

^{13}C NMR (75.5 MHz, 293 K, $CDCl_3$):

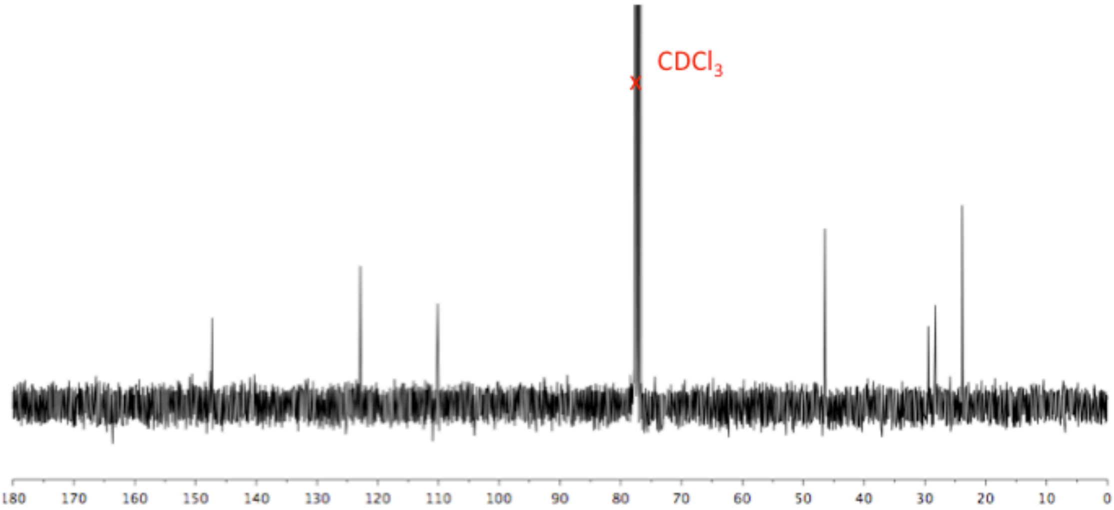

Phenyl-linked tetra-triazole macrocycle 2

^{1}H NMR (300 MHz, 293 K, d$_6$-DMSO):

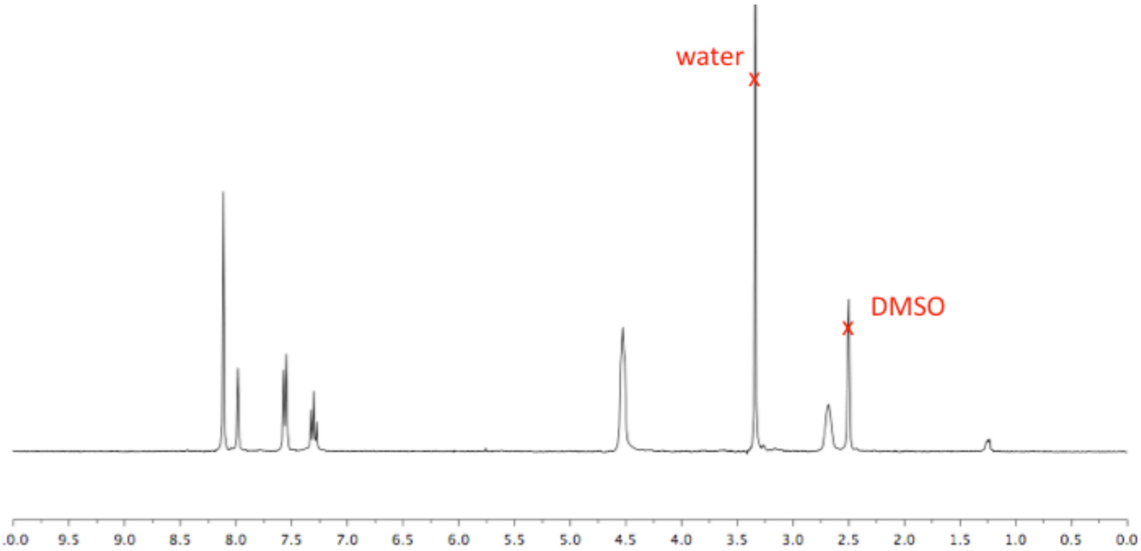

^{13}C NMR (75.5 MHz, 293 K, d$_6$-DMSO):

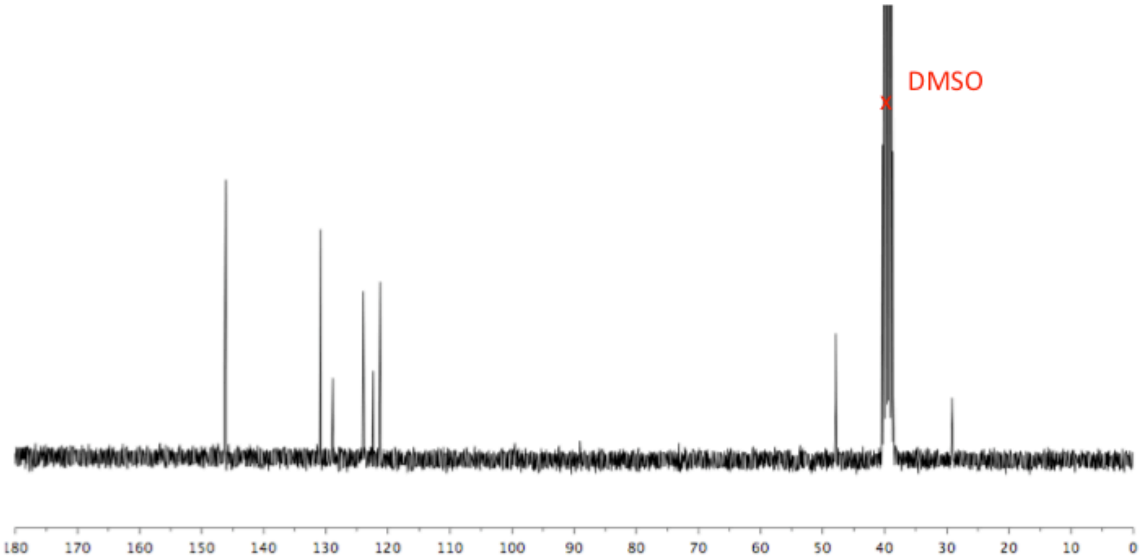

Pyridyl-linked tetra-triazole macrocycle 3

^{1}H NMR (500 MHz, 293 K, d$_6$-DMSO):

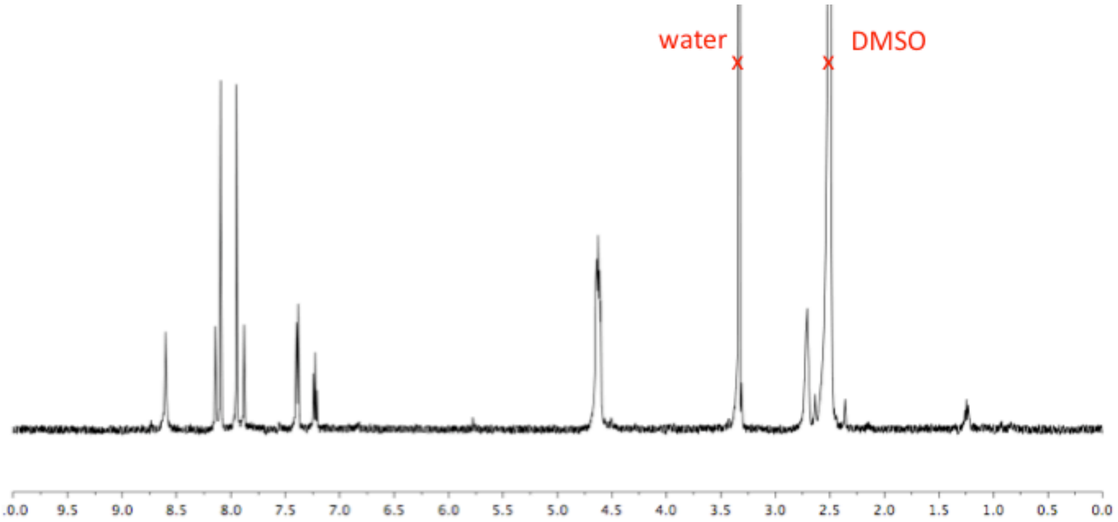

^{13}C NMR (75.5 MHz, 293 K, d$_6$-DMSO):

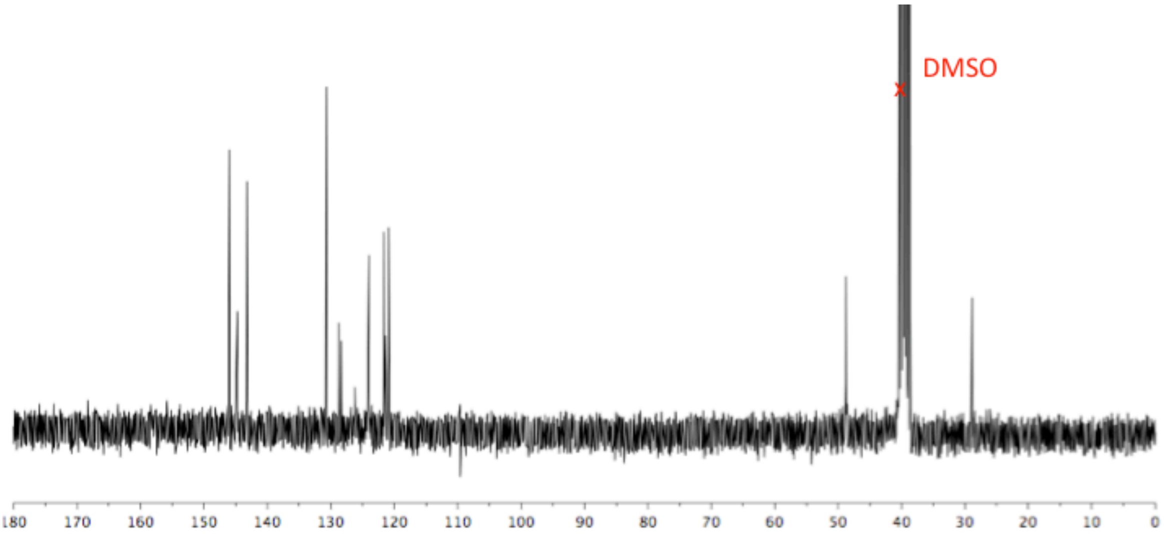

Tetra-triazolium macrocycle tetrafluoroborate 7·4BF$_4$

^{1}H NMR (500 MHz, 293 K, d$_6$-DMSO):

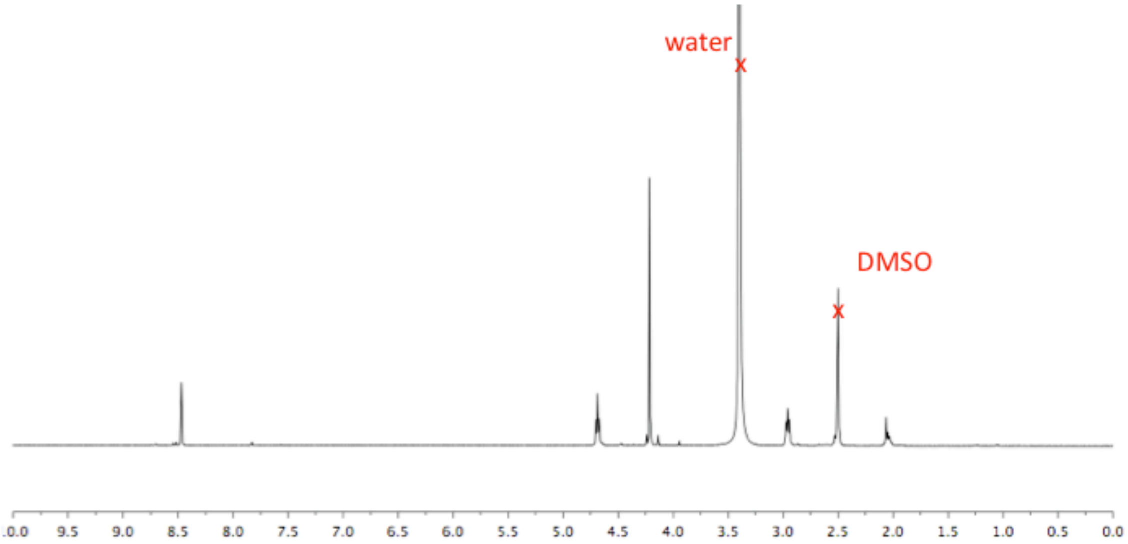

^{13}C NMR (500 MHz, 293 K, d$_6$-DMSO):

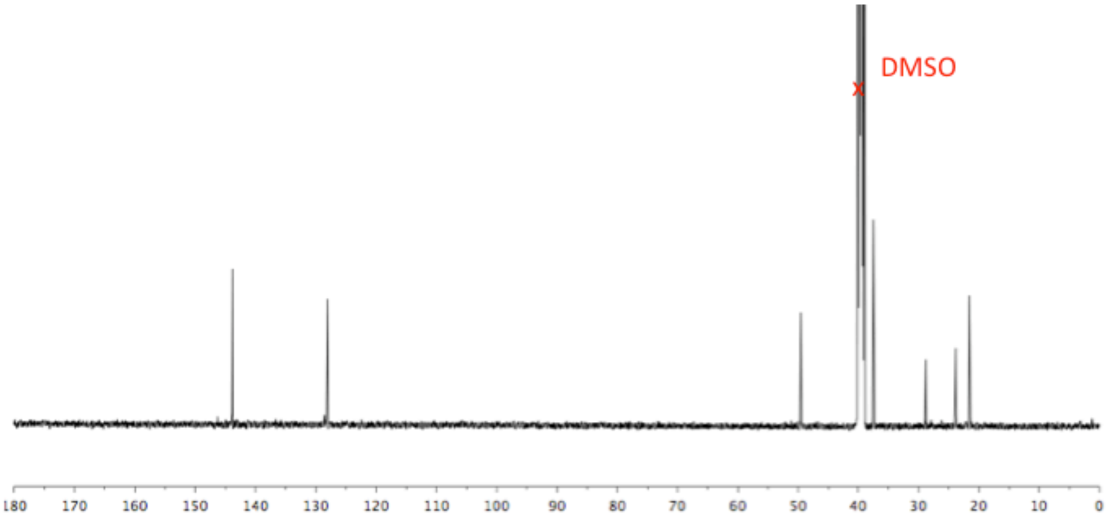

Gas Phase Molecular Modelling

The structure of each anion complex was selected through the cluster analysis of a trajectory file composed of 50000 frames obtained as described below. The structures of the most populated clusters determined for monoatomic anions display similar binding arrangements with the anion positioned in the middle of **7**, which adopts a flattened bowl-shaped conformation with four triazolium moieties slightly tilted relative to the macrocyclic plane, defined by the nitrogen atoms directly linked to the propyl spacers. In addition, the C-H protons from the four triazolium rings point towards the anion at average distances of H···F^- (2.68 Å), H···Cl^- (2.82 Å), H···Br^- (2.92 Å) and H···I^- (3.10 Å), consistent with the existence of C-H···anion hydrogen bonding interactions.[S2] This binding arrangement is illustrated in Figure S1 with representative structures of fluoride and iodide complexes.

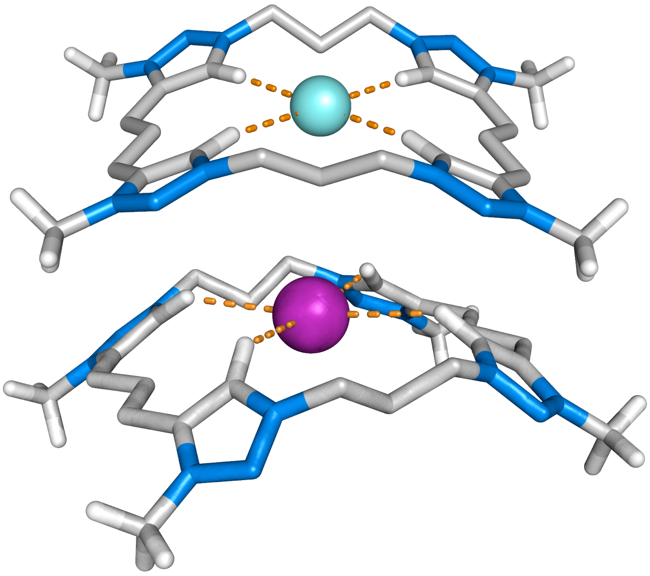

Fig. S1. Representative molecular mechanics structures of **7**·F (top) and **7**·I (bottom) complexes showing the smallest and largest halide anions establishing charge-assisted C-H···anion hydrogen bonding interactions with four triazolium rings.

The most populated cluster for the sulfate complex revealed a different binding scenario than described earlier for the monoatomic anions. As depicted in Figure S2, the oxo-anion is entirely inserted into the macrocyclic cavity with two oxygen atoms bridging to two opposite triazolium rings through two C-H···O charged assisted hydrogen bonds with average distances of 2.50 and 2.47 Å. Furthermore, the remaining two triazolium rings adopt an oblique spatial disposition suggesting the existence of π-anion interactions at 2.87 and 3.12 Å.

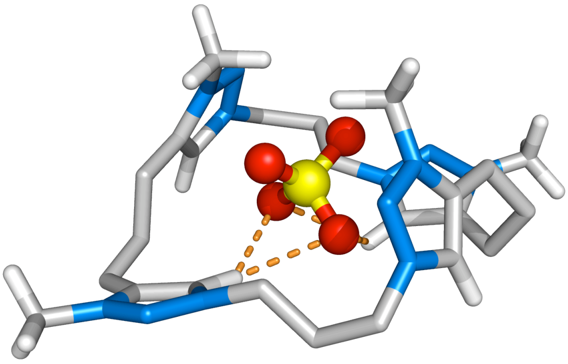

Fig. S2. Molecular mechanics structure of sulfate complex showing the anion inserted into the macrocyclic cavity stabilised by two C-H···O hydrogen-bond bridges.

Experimental Details for Molecular Modelling

All MD and QM/MM simulations were carried out with the AMBER 11 suite of programs.[S3]

The parameters for the classical MD simulations for the macrocycle were taken from the General Amber Force Field (GAFF).[S4] The fluoride, chloride, bromide and iodide anions, with charge of –1, were described with van der Waals parameters taken from the literature.[S5] For the SO_4^{2-} anion and BF_4^- counter-ion, the atomic point charges were obtained according to the RESP methodology[S6] on the electrostatic potential calculated at the HF/6-31G* level of theory with Gaussian09.[S7] The force field parameters for SO_4^{2-} were taken from the GAFF and for BF_4^- from ref. S8. The DMSO solvent molecules were described using a full atom model with atomic charges and force field parameters taken from ref. S9. The TIP3P model was used for the water molecules.[S10]

In order to obtain atomic charges less dependent of the molecular conformation or orientation of macrocycle, the calculation of RESP charges of **7** employed in the MD simulations was preceded by conformational analysis using AM1-BCC charges [S11] and the X-ray structure as a starting conformation. This structure was minimized by molecular mechanics and subsequently heated in gas phase at 1000 K for 50 ps, followed by a collection run of 5 ns, using a time step of 1 fs. Frames were saved every 0.1 ps leading to a trajectory file containing 50000 structures. The high temperature ensured that all conformational barriers were surmounted, enabling the **7** to cover all the conformational space. Afterwards, all these structures were minimized by MM using a steepest descendent gradient followed by the conjugate gradient algorithm, until convergence criteria of 0.0001 kcal mol^{-1} $Å^{-1}$ were attained. The optimised structures were energy sorted and four lowest energy ones defined by different spatial orientations of the successive triazolium protons relative to the macrocyclic plane (++++, +++-, ++--, +-+-, with + and – meaning that a triazolium proton is below or above the macrocyclic plane, respectively) plus the X-ray structure, were appointed for HF/6-31G* geometry optimizations and ESP calculations as described above. The individual ESP data were extracted from the corresponding Gaussian 09[S7] output and then the ESP data of the five conformations were concatenated and subsequently used to generate the input files for the two-stage RESP fitting using identical weights for all conformations.

The docking between the anions and **7** with RESP charges was also carried out in the gas phase by quenched molecular dynamics using the protocol used for the free macrocycle.

A representative structure of the more populated cluster determined for each anion complex was solvated *via* PACKMOL[S12] with a cubic box containing a random distribution composed of 458 all atom DMSO and 1800 TIP3P water molecules, consistent with the v/v DMSO/H_2O (1:1) solvent mixture ratio. The charge neutrality of each system was achieved by addition of an appropriate number of BF_4^- anions. Subsequently, each system was equilibrated under periodic boundary conditions as follows. The equilibration process started with the minimization of the solvent molecules by molecular mechanics keeping the solute fixed with a positional restraint of 500 kcal mol^{-1} $Å^{-2}$. Then, the restraint was removed and the entire system was allowed to relax. The system was then heated to 300 K for 100 ps with a weak positional restraint (10 mol^{-1} $Å^{-2}$) on the solute using the Langevin thermostat with a collision frequency of 1 ps^{-1} in an NVT ensemble. The positional restraint was definitively removed and the system was allowed to equilibrate in a NPT ensemble at 1 atm for 200 ps using isotropic pressure scaling and a relaxation time of 2 ps. The simulation was continued for 20.8 ns. Bond lengths involving all bonds to hydrogen atoms were constrained with the SHAKE algorithm.[S13] The Newton equations of motion were integrated with a 2 fs time step. Particle Mesh Ewald method[S14] was used to treat the long-range electrostatic interactions and the non-bonded van der Waals interactions were truncated with a 10 Å cut-off.

For the QM/MM simulations, each system was divided into two parts. The QM region comprising the anion complex was treated by the semi-empirical PM3 Hamiltonian while the DMSO and water solvent molecules together with BF_4^- counter-ions were treated by a classical MM potential using force field parameters as described earlier. The starting configuration of a given system was the initial structures used in the corresponding classical MD simulation. The QM/MM simulations were performed under periodic boundary conditions using the Sander module of the AMBER 11. A 10 Å cut-off was used for both regions. A Particle Mesh Ewald method (PME) modified for QM/MM systems was applied to calculate the long- range QM-QM and QM-MM electrostatic interactions.[S15] The SHAKE algorithm was also used in conjugation with a 2 fs time step. The systems were equilibrated as described for classical MD simulations. Subsequently, a NPT production run (300 K, 1 atm) was performed over 2 ns and snapshots were saved to a trajectory every 1 ps. The collected data were analyzed with the PTRAJ module as implemented in the Amber package. Molecular diagrams were drawn with PyMOL.[S16]

References

[S1] M. J. Hynes, J. Chem. Soc., Dalton Trans., **1993**, 311.

[S2] A. Kovács, Z. Varga, *Chem. Soc. Rev.,* **2006**, 710-727.

[S3] D. A. Case, T. A. Darden, T. E. Cheatham III, C. L. Simmerling, J. Wang, R. E. Duke, R. Luo, M. Crowley, R. C . Walker, W. Zhang, K. M. Merz, B. Wang, S. Hayik, A. Roitberg, G. Seabra, I. Kolossváry, K. F. Wong, F. Paesani, J. Vanicek, X. Wu, S. R. Brozell, T. Steinbrecher, H. Gohlke, L. Yang, C. Tan, J. Mongan, V. Hornak, G. Cui, D. H. Mathews, M. G. Seetin, C. Sagui, V. Babin, P. A. Kollman. *AMBER 11*, University of California: San Francisco, **2010**.

[S4] J. Wang, R. M. Wolf, J. W. Caldwell, P. A. Kollman, D. A. Case, *J. Comput. Chem.* **2004**, *25*, 1157-1174.

[S5] I. S. Joung, T. E. Cheatham III, *J. Phys. Chem. B,* **2008**, *112*, 9020-9041.

[S6] R C. I. Bayly, P. Cieplak, W. D. Cornell, P. A. Kollman, *J. Phys. Chem.* **1993**, *97*, 10269-10280.

[S7] Gaussian 09, Revision A.1, M. J. Frisch, G. W. Trucks, H. B. Schlegel, G. E. Scuseria, M. A. Robb, J. R. Cheeseman, G. Scalmani, V. Barone, B. Mennucci, G. A. Petersson, H. Nakatsuji, M. Caricato, X. Li, H. P. Hratchian, A. F. Izmaylov, J. Bloino, G. Zheng, J. L. Sonnenberg, M. Hada, M. Ehara, K. Toyota, R. Fukuda, J. Hasegawa, M. Ishida, T. Nakajima, Y. Honda, O. Kitao, H. Nakai, T. Vreven, J. A. Montgomery, Jr., J. E. Peralta, F. Ogliaro, M. Bearpark, J. J. Heyd, E. Brothers, K. N. Kudin, V. N. Staroverov, R. Kobayashi, J. Normand, K. Raghavachari, A. Rendell, J. C. Burant, S. S. Iyengar, J. Tomasi, M. Cossi, N. Rega, J. M. Millam, M. Klene, J. E. Knox, J. B. Cross, V. Bakken, C. Adamo, J. Jaramillo, R. Gomperts, R. E. Stratmann, O. Yazyev, A. J. Austin, R. Cammi, C. Pomelli, J. W. Ochterski, R. L. Martin, K. Morokuma, V. G. Zakrzewski, G. A. Voth, P. Salvador, J. J. Dannenberg, S. Dapprich, A. D. Daniels, Ö. Farkas, J. B. Foresman, J. V. Ortiz, J. Cioslowski, and D. J. Fox, Gaussian, Inc., Wallingford CT, 2009.

[S8] J. Andrade, E. S. Böes, H. Stassen, *J. Phys. Chem. B,* **2002**, *106*, 13344-13351.

[S9] T. Fox, P. A. Kollman, *J. Chem Phys. B* **1998**, *102*, 8070-8079.

[S10] W. L. Jorgensen, J. Chandrasekhar, J. D. Madura, R. Impey, M. L. Klein, *J. Chem. Phys.* **1983**, *79*, 926-935.

[S11] A. Jakalian, B. L. Bush, D. B. Jack, C. I. Bayly, *J. Comput. Chem.*, **2000**, *21*(2), 132–146.

[S12] L. Martínez, R. Andrade, E. G. Birgin, J. M. Martínez, *J. Comput. Chem.* **2009**, *30*(13), 2157-2164.

[S13] J. P. Ryckaert, G. Ciccotti, H. J. C. Berendsen, *J. Comput. Phys.* **1977**, *23*, 327-341.

[S14] U. Essmann, L Perera, M. L. Berkowitz, T. Darden, H. Lee, L. G. Perdensen, *J. Chem. Phys.* **1995**, *103*, 8577-8593.

[S15] K. Nam, J. L. Gao, D. M. York, *J. Chem. Theory and Comput.*, **2005**, *1*, 2–13.

[S16] PyMOL Molecular Graphics System, Version 1.2r2, DeLano Scientific LLC, **2009**.